NASA TECHNICAL MEMORANDUM

NASA TM X-3180

NASA TM X-3180

COLD-AIR ANNULAR-CASCADE INVESTIGATION OF AERODYNAMIC PERFORMANCE OF COOLED TURBINE VANES

II - Trailing-Edge Ejection, Film Cooling, and Transpiration Cooling

Louis J. Goldman and Kerry L. McLallin

Lewis Research Center

Cleveland, Ohio 44135

NATIONAL AERONAUTICS AND SPACE ADMINISTRATION • WASHINGTON, D. C. • JANUARY 1975

1. Report No. NASA TM X-3180	2. Government Accession No.	3. Recipient's Catalog No.
4. Title and Subtitle COLD-AIR ANNULAR-CASCADE INVESTIGATION OF AERODYNAMIC PERFORMANCE OF COOLED TURBINE VANES. II - TRAILING-EDGE EJECTION, FILM COOLING, AND TRANSPIRATION COOLING		5. Report Date January 1975 6. Performing Organization Code
7. Author(s) Louis J. Goldman and Kerry L. McLallin		8. Performing Organization Report No. E-8049 10. Work Unit No. 505-04
9. Performing Organization Name and Address Lewis Research Center National Aeronautics and Space Administration Cleveland, Ohio 44135		11. Contract or Grant No. 13. Type of Report and Period Covered Technical Memorandum
12. Sponsoring Agency Name and Address National Aeronautics and Space Administration Washington, D.C. 20546		14. Sponsoring Agency Code

15. Supplementary Notes

16. Abstract

The aerodynamic performance of four different cooled vane configurations was experimentally determined in a full-annular cascade at a primary- to coolant-total-temperature ratio of 1.0. The vanes were tested over a range of coolant flow rates and pressure ratios. Overall vane efficiencies were obtained and compared, where possible, with the results obtained in a four-vane, annular-sector cascade. The vane efficiency and exit flow conditions as functions of radial position were also determined and compared with solid (uncooled) vane results.

17. Key Words (Suggested by Author(s))	18. Distribution Statement
Aerodynamic performance Cooled turbine vanes	Unclassified - unlimited STAR category 02 (rev.)

19. Security Classif. (of this report)	20. Security Classif. (of this page)	21. No. of Pages	22. Price*
Unclassified	Unclassified	35	$3.75

* For sale by the National Technical Information Service, Springfield, Virginia 22151

COLD-AIR ANNULAR-CASCADE INVESTIGATION OF AERODYNAMIC PERFORMANCE OF COOLED TURBINE VANES II - TRAILING-EDGE EJECTION, FILM COOLING, AND TRANSPIRATION COOLING

by Louis J. Goldman and Kerry L. McLallin

Lewis Research Center

SUMMARY

The aerodynamic performance of four different cooled vane configurations was experimentally determined in a full-annular cascade, where three-dimensional effects could be obtained. The vanes were tested over a range of coolant flow rates to about 6 percent of the primary flow at a primary- to coolant-total-temperature ratio of 1.0. Tests were conducted at pressure ratios that corresponded to mean-radius ideal aftermixed critical velocity ratios of 0.71 and 0.86. The design value for the vanes is 0.87. Overall vane efficiencies were obtained for these critical velocity ratios and compared, where possible, with the corresponding four-vane cascade results. The vane efficiency and exit flow conditions as functions of radial position were also obtained and compared with the solid (uncooled) vane results.

In general, it was found that increasing the coolant flow rate resulted in an increase in primary efficiency and a decrease in thermodynamic efficiency. Primary efficiency was found to be independent of the ideal aftermixed critical velocity ratio, while thermodynamic efficiency decreased with decreasing ideal aftermixed critical velocity ratio. The thermodynamic efficiency as a function of radial position was found to be modified by the addition of coolant, particularly near the end walls. However, no trend with coolant flow was noted for aftermixed flow angle and aftermixed static-pressure to inlet-total-pressure ratio. Good agreement between the full-annular and four-vane cascade results was obtained for overall thermodynamic efficiency, but significant differences were noted for overall primary efficiency. For a given coolant flow rate, the highest overall efficiency was obtained for the trailing-edge-ejection vane, and the lowest for the transpiration-cooled vane.

INTRODUCTION

The use of cooled turbine vanes and blades for advanced high-temperature aircraft engines has resulted in a program of cooling studies at the Lewis Research Center. One aspect of this program is the determination of the effect of different vane cooling schemes on the performance of turbine vanes having the same aerodynamic profile. Some of these results obtained in a four-vane annular-sector cascade are reported in references 1 and 2. Static and total pressures measured at the vane exit are presented in reference 1 for the solid (uncooled) vane which serves as the basis for comparison of the different cooling configurations. It was found that the radial pressure gradient was significantly lower than would be expected for three-dimensional flow. In reference 2 the aerodynamic performance of the solid vane, as well as the performance of two different cooling configurations tested at primary- to coolant-total-temperature ratios of 1.0, 1.75, and 2.75, is reported. However, only two cooling configurations were tested, and the results that were obtained are somewhat limited since true three-dimensional gradients could not be adequately simulated.

An investigation was, therefore, undertaken wherein additional cooled vane configurations, as well as those tested in the four-vane cascade, would be studied in a full-annular cascade, where valid three-dimensional effects could be obtained. The full-annular cascade was designed primarily for cold-air studies at a primary- to coolant-total-temperature ratio of 1.0. This enabled the cascade to be manufactured and operated more economically than would have been possible at higher temperature ratios. It was felt that a valid comparison of the cooled configurations could still be made at this low temperature ratio, since the total-temperature ratio affects the level of efficiency but not the basic trends (ref. 2).

The first phase of the investigation was concerned with the performance of the solid vanes, and the results are reported in reference 3. It was found that the efficiency for the vane passage obtained in the full-annular cascade agreed well with those obtained in the four-vane cascade. The second phase of the investigation, which is the subject of this report, presents the experimental results for the following cooled vane configurations: (1) trailing-edge ejection, (2) trailing-edge ejection plus forward film-cooling, (3) trailing-edge ejection plus rearward film-cooling, and (4) transpiration cooling. Only the latter two configurations were tested in the four-vane cascade.

Performance data were obtained in the full-annular cascade over a range of coolant flow rates to about 6 percent of the primary flow at a primary- to coolant-total-temperature ratio of 1.0. The cooled vanes were tested at pressure ratios that correspond to mean-radius ideal aftermixed critical velocity ratios of 0.71 and 0.86. The design value for the vanes is 0.87. Vane efficiencies were obtained for these critical velocity ratios and compared, where possible, with the corresponding four-vane cascade

results. The vane efficiency and exit flow conditions as functions of radial position are also presented and compared with the solid (uncooled) vane results.

The work presented herein was conducted in the U.S. customary system of units. Conversion to the International System of Units (SI) was done for reporting purposes only.

APPARATUS AND PROCEDURE

Cascade Facility

The full-annular cascade facility consists essentially of an inlet section, a test section, and an exit section. The actual facility and a schematic cross-sectional view are shown in figures 1 and 2, respectively. The facility is described fully in reference 3. In operation, atmospheric primary air is drawn through the inlet section, the blading, and the exit section and then exhausted through the laboratory altitude exhaust system. Vane cooling air, provided by the laboratory combustion air system, passes through the cooling passages of the test vanes and then mixes with the primary air prior to entering the exhaust system.

The inlet section, consisting of a bellmouth and a short straightening section, was designed to accelerate the flow to uniform parallel flow conditions at the vane inlet. The test section consists of a sector of five vanes which are part of the full-annular ring of 72 vanes. These five vanes are provided with cooling air. The remaining vanes are solid and have the same aerodynamic profile as the cooled vanes. The coordinates of the vane profile are given in references 1 and 2. The twisted vane has a height of 9.78 centimeters (3.85 in.) and an axial chord of 5.08 centimeters (2.00 in.) at the mean radius. The different cooled vane configurations tested are shown in figure 3; schematic cross-sectional views of these vanes are shown in figure 4. The exit section consists of a diffusing section and a flow-straightening section. Because of mechanical failure, the diffuser was removed for this investigation (fig. 2). This resulted in a more rapid deceleration of the flow but did not seem to affect cascade operation.

Instrumentation

Instrumentation was provided to measure wall static pressures at various locations, survey probe data downstream of the test vanes, and coolant flow rate to the test vanes. Figure 2 shows the station nomenclature used for this instrumentation.

Static pressures were measured at stations 1, 2, and 3 by taps located on the inner (hub) and outer (tip) walls of the cascade (fig. 2). The circumferential locations of the taps are given in reference 3. These measurements were used to ascertain the uniformity of the flow as it passed through the cascade. In addition, static pressure taps were located approximately 2 axial chord lengths downstream of the vanes, where the flow was assumed to be mixed to uniform conditions (station 3M). This pressure was used to set the primary flow in the cascade.

A calibrated survey probe was located 1.27 centimeters (1/2 in.) downstream of the test vanes, as shown in figure 5. The probe was positioned at a fixed angle of 64° from the axial direction, which corresponds to the design flow angle at the mean radius. The probe could travel circumferentially over the middle three of the five test vanes, with the radial position being limited primarily by probe geometry to the survey area shown in figure 5. The survey probe was used to obtain the total pressure, total temperature, static pressure, and flow angle. The probe is shown in figure 6. All pressures were measured with calibrated strain-gage pressure transducers. A Chromel-Alumel aspirated thermocouple was used to obtain the total temperature. All the instrumentation has been described in more detail in reference 3.

The coolant flow rate was measured by use of various-size calibrated Venturi meters. The Venturi meters and runs conformed with ASME specifications and were calibrated prior to use. Venturi meters were used instead of orifice plates to minimize the total pressure loss of the coolant and thereby allow higher coolant flow rates to be obtained.

Procedure

In order to operate the cascade facility, atmospheric primary air from the test cell was drawn through the cascade and exhausted into the laboratory altitude exhaust system. The test conditions were set by controlling the pressure ratio across the vane row with two different-size throttle valves located in the exhaust system. Static pressure taps located downstream of the test section, where the flow was assumed to be circumferentially uniform (station 3M), were used to set this pressure ratio. Vane cooling air at room temperature was provided by the laboratory combustion air system. The desired coolant flow rate was obtained by setting the upstream Venturi pressure with a pressure regulator and the Venturi pressure ratio with a throttling valve located downstream of the Venturi run.

The cooled vanes were tested at primary-air pressure ratios that corresponded to mean-radius ideal aftermixed critical velocity ratios of 0.71 and 0.86. The design value for the vanes is 0.87. Coolant flow rates to 6 percent of the primary flow were

investigated. At a given flow condition, probe survey data were obtained at a number of different radii over the vane height. At any fixed radius, the probe was moved circumferentially over three vane passages, with survey data being obtained continuously. The slow speed of the circumferential drive mechanism, coupled with the data recording rate, resulted in survey data being obtained at approximately 0.04° increments. The vane spacing Θ in the cascade was 5°. (All symbols are defined in appendix A.) The output signals of the thermocouple and pressure transducers were digitized and recorded on magnetic tape.

Data Reduction

The cooled vane performance presented herein was calculated from the exit survey probe measurements (total pressure, total temperature, static pressure, flow angle, and probe position) and the measured coolant flow rate. Data from the middle wake (of the three wakes that were measured) were used in these calculations. It was assumed that no loss of total pressure or temperature occurred between the bellmouth inlet (station 0) and the vane inlet (station 1).

The calculation of the vane efficiencies is based on the determination of a hypothetical state where it is assumed that the flow has mixed to a circumferentially uniform condition. The application of the conservation equations to an annular-sector control volume to obtain this aftermixed state, at each radius, has been described fully in reference 3. The aftermixed vane efficiency is used herein because it is theoretically independent of the axial location of the survey measurement plane. It should be noted that the aftermixed efficiency contains not only the vane profile loss, but also the mixing loss.

For cooled vane performance, both the thermodynamic and primary efficiencies are in general use. Thermodynamic efficiency is defined as the ratio of the actual aftermixed kinetic energy to the sum of the ideal aftermixed kinetic energies of both the primary and coolant flows. Primary efficiency is defined as the ratio of the actual aftermixed kinetic energy to the ideal aftermixed kinetic energy of the primary flow only. The thermodynamic efficiencies at a given radius $\overline{\eta}_{3M,\,T}(r)$ and for the total passage $\overline{\overline{\eta}}_{3M,\,T}$ are given by

$$\overline{\eta}_{3M,\,T}(r) = \frac{V_{3M}^2(r)}{y_p(r)\left[V_{3M,\,id}^2(r)\right]_p + y_c(r)\left[V_{3M,\,id}^2(r)\right]_c} \tag{1}$$

$$\bar{\bar{\eta}}_{3M,T} = \frac{\int_{r_i}^{r_o} \left[\rho_{3M}(r) V_{3M,z}(r) V_{3M}^2(r)\right] r\, dr}{\int_{r_i}^{r_o} \rho_{3M}(r) V_{3M,z}(r) \left\{ y_p(r) \left[V_{3M,id}^2(r)\right]_p + y_c(r) \left[V_{3M,id}^2(r)\right]_c \right\} r\, dr} \tag{2}$$

where the ideal velocities of the primary $\left[V_{3M,id}(r)\right]_p$ and coolant flows $\left[V_{3M,id}(r)\right]_c$ are given by

$$\left[V_{3M,id}(r)\right]_p = \sqrt{\left(\frac{2\gamma}{\gamma - 1}\right) gRT_1' \left\{1 - \left[\frac{p_{3M}(r)}{p_1'}\right]^{(\gamma-1)/\gamma}\right\}} \tag{3}$$

$$\left[V_{3M,id}(r)\right]_c = \sqrt{\left(\frac{2\gamma}{\gamma - 1}\right) gRT_c' \left\{1 - \left[\frac{p_{3M}(r)}{p_c'}\right]^{(\gamma-1)/\gamma}\right\}} \tag{4}$$

The fraction of coolant flow to total flow $y_c(r)$ is assumed to be independent of radius r and to equal

$$y_c = \frac{\bar{\bar{m}}_c}{\bar{\bar{m}}} = 1 - y_p = \text{Constant} \tag{5}$$

where $\bar{\bar{m}}_c$ is the measured coolant flow rate per passage and $\bar{\bar{m}}$ is the total flow rate per passage given by

$$\bar{\bar{m}} = \int_{r_h}^{r_t} \int_0^{\Theta} \rho_3(r, \theta) V_{3,z}(r, \theta) r\, d\theta\, dr \tag{6}$$

The primary efficiencies at a given radius $\bar{\eta}_{3M,p}(r)$ and for the total passage $\bar{\bar{\eta}}_{3M,p}$ are given by

$$\bar{\eta}_{3M,p}(r) = \frac{V_{3M}^2(r)}{y_p \left[V_{3M,id}^2(r)\right]_p} \tag{7}$$

$$\bar{\bar{\eta}}_{3M,p} = \frac{\int_{r_i}^{r_o} \left[\rho_{3M}(r) V_{3M,z}(r) V_{3M}^2(r)\right] r \, dr}{\int_{r_i}^{r_o} \left\{ y_p \rho_{3M}(r) V_{3M,z}(r) \left[V_{3M,id}^2(r)\right]_p \right\} r \, dr} \tag{8}$$

RESULTS AND DISCUSSION

A cold-air experimental investigation was conducted in a full-annular cascade to determine the effect of different vane cooling configurations on the performance of turbine vanes having the same aerodynamic profile. Tests were conducted on four different cooling configurations over a range of coolant flow rates to about 6 percent of the primary flow. The cooled vanes were tested at pressure ratios that corresponded to mean-radius ideal aftermixed critical velocity ratios of 0.71 and 0.86. The design value for the vanes is 0.87. Overall vane efficiencies were obtained at these critical velocity ratios and compared where possible with the results obtained in a four-vane annular-sector cascade. The vane exit flow conditions and efficiency as functions of radial position are also presented and compared with the results from the solid (uncooled) vane tests. The results for the four cooled vane configurations are presented first, and then a comparison is made of the different cooling configurations.

Trailing-Edge Ejection

The overall aftermixed efficiencies with trailing-edge ejection are shown in figure 7 as a function of coolant flow rate and ideal critical velocity ratio. Increasing the coolant flow rate resulted in an increase in primary efficiency and a decrease in thermodynamic efficiency. Essentially, the primary efficiency increased with increased coolant flow because the ideal kinetic energy of the coolant was not accounted for in this definition of efficiency. The primary efficiency is seen to be independent of the ideal aftermixed critical velocity ratio. Similar trends have been reported in reference 4 for various trailing-edge slot geometries.

The thermodynamic efficiency was, however, dependent on the ideal aftermixed critical velocity ratio. Decreasing the ideal critical velocity ratio (which increased the exit static pressure) required a higher coolant total pressure for the same coolant fraction. The higher coolant total pressure resulted in a larger ratio of coolant ideal kinetic energy to primary ideal kinetic energy, which tended to decrease the thermodynamic efficiency.

The aftermixed thermodynamic efficiency and the aftermixed flow conditions with trailing-edge ejection are shown in figures 8 and 9, respectively, as a function of radial position. Results are shown for an ideal aftermixed critical velocity ratio of 0.86 and for coolant flow rates of 0, 2.95, and 5.34 percent. For comparison the solid (uncooled) vane results are shown as a solid line in these figures. Increasing the coolant flow rate decreased the thermodynamic efficiency level and modified the efficiency variation with radial position. The difference between the solid-vane and zero-percent-coolant-flow results was due to recirculation of some of the primary flow through the trailing-edge slots caused by the radial pressure gradient at the vane exit. The aftermixed flow angle and the aftermixed static-pressure to inlet-total-pressure ratio as a function of radial position (fig. 9) were similar to those obtained with the solid (uncooled) vane, except that the level of the flow angle was somewhat lower. No particular trend with coolant flow rate is noted for the aftermixed flow conditions.

Trailing-Edge Ejection Plus Forward Film-Cooling

The overall aftermixed efficiencies with trailing-edge ejection plus forward film-cooling are shown in figure 10 as a function of coolant flow rate and ideal critical velocity ratio. The variation of primary and thermodynamic efficiency with coolant flow and critical velocity ratio followed the same trends as those observed for the trailing-edge ejection vanes in figure 7.

The aftermixed thermodynamic efficiency and the aftermixed flow conditions with trailing-edge ejection plus forward film-cooling are shown in figures 11 and 12, respectively, as a function of radial position. Results are shown for an ideal aftermixed critical velocity ratio of 0.86 and for coolant flow rates of 0, 3.36, and 4.80 percent. The efficiency variation with radial position was strongly affected by coolant addition, particularly in the hub region. The aftermixed flow conditions showed almost no effect of coolant addition, being similar to the results obtained for the trailing-edge-ejection vanes.

Trailing-Edge Ejection Plus Rearward Film-Cooling

The overall aftermixed efficiencies with trailing-edge ejection plus rearward film-cooling are shown in figure 13 as a function of coolant flow rate and ideal critical velocity ratio. These results were obtained with the leading-edge impingement coolant supply sealed off (fig. 4). This was necessary since no provision was made in the cascade to exhaust this flow properly. The performance results reported for the four-vane cascade

(ref. 2) were obtained with the impingement coolant supply open. However, enough information is provided in reference 2 so that the performance with the supply sealed off can be estimated. The basic assumption necessary to make this estimation is that at a constant coolant- to primary-total-pressure ratio, the only effect of having the leading-edge impingement coolant supply open is to increase the total coolant flow by the amount going through the leading-edge passage. This is reasonable since in reference 2 the leading-edge impingement coolant was mixed with the primary flow downstream of the survey plane. Therefore, it did not affect the measured velocity level. The calculation procedure is described in appendix B. Both the original and estimated four-vane-cascade results are shown in figure 13.

The aftermixed efficiencies obtained in the full-annular cascade and the four-vane cascade showed the same trends with coolant flow. The thermodynamic efficiency levels were about the same, but the primary efficiency levels were different. This was due, possibly, to the manufacturing tolerances of the different vanes (with the same cooling configuration) that were used in the two cascades. Unfortunately, the vanes tested in the four-vane cascade were not available for testing in the full-annular cascade. During testing it was observed that to obtain the same coolant flow rate as in the four-vane cascade, a higher coolant- to primary-total-pressure ratio was required. This was apparently caused by differences in the internal cooling passages and cooling slot areas of the two sets of vanes.

Results were also obtained for this cooling configuration with the suction surface slots sealed. These results are represented by solid symbols in figure 13. For a given coolant fraction, sealing the suction surface slots resulted in an increase in aftermixed efficiency and also required a larger coolant- to primary-total-pressure ratio than for the open suction surface slot configuration. The larger coolant total pressure must therefore result in an increase in the measured kinetic energy (eq. (7)). Since the ideal kinetic energy of the coolant also increased, the effect on thermodynamic efficiency (eq. (1)) was less pronounced than that observed for primary efficiency.

The aftermixed thermodynamic efficiency and aftermixed flow conditions with trailing-edge ejection plus rearward film-cooling are shown in figures 14 and 15, respectively, as a function of radial position. Results are shown for an ideal aftermixed critical velocity ratio of 0.86 and coolant flow rates of 0, 3.26, and 4.34 percent. The efficiency variation with radial position was affected by coolant addition, particularly in the tip region. The effect of coolant flow on the aftermixed flow conditions is similar to those found previously for the other cooling configurations. Results shown in figures 14 and 15 with the suction surface slots sealed and opened, at essentially the same coolant flow rate, indicate that the flow from the suction surface slots did not significantly modify the variation of efficiency and flow conditions with radial position.

Transpiration Cooling

The overall aftermixed efficiencies with transpiration cooling are shown in figure 16 as a function of coolant flow rate and ideal critical velocity ratio. Increasing the coolant flow rate resulted in a very large decrease in thermodynamic efficiency and only a slight increase in primary efficiency. This behavior was typical and resulted from the fact that the coolant was ejected normal to the vane surface and therefore could not effectively add its kinetic energy to the primary flow. The results obtained in the four-vane cascade are also shown in figure 16. Good agreement between the two cascades was obtained for thermodynamic efficiency, but large differences are noted for primary efficiency. The reasons for these differences in primary efficiency are not known. It is felt that they may have been caused by partial plugging, particularly on the suction surface, of the 0.0025-centimeter (0.001-in.) pores which constitute the cooling passages of these vanes.

The aftermixed thermodynamic efficiency and aftermixed flow conditions with transpiration cooling are shown in figures 17 and 18, respectively, as a function of radial position. Results are shown for an ideal aftermixed critical velocity ratio of 0.86 and for coolant flow rates of 0 and 2.85 percent. The coolant flow is seen to have a large effect on the efficiency variation with radial position but almost no effect on the aftermixed flow conditions.

Comparison of Different Cooling Configurations

The overall aftermixed efficiency as a function of coolant flow rate is shown in figure 19 for the four cooling configurations tested. At a given coolant flow rate, the highest efficiency was obtained for the trailing-edge-ejection vane, and the lowest for the transpiration-cooled vane. This had been expected, since the coolant flow from the trailing-edge-ejection vane was discharged in the direction of the primary flow and therefore could very effectively add its kinetic energy to that of the primary flow. As explained previously, the coolant from the transpiration vane was discharged normal to the primary flow direction and therefore its kinetic energy was essentially lost.

An interesting comparison of the two film-cooled vanes is noted in figure 19. On the basis of the primary efficiency, the performances of the two vanes were almost identical and just slightly lower than the performance of the trailing-edge-ejection vane. The thermodynamic efficiency, however, indicated a higher performance for the vane with forward film-cooling. The reason for this is that, for a given coolant flow rate, each cooling configuration required a different coolant- to primary-total-pressure ratio (since the coolant slot areas are different). In particular, the vane with forward film-

cooling required a lower coolant total pressure than did the vane with rearward film-cooling. This resulted in a smaller ideal kinetic energy of the coolant and therefore a higher thermodynamic efficiency (for constant primary efficiency).

SUMMARY OF RESULTS

The aerodynamic performance of four different cooled vane configurations was experimentally determined in a full-annular cascade, where three-dimensional effects could be obtained. The configurations tested were (1) trailing-edge ejection, (2) trailing-edge ejection plus forward film-cooling, (3) trailing-edge ejection plus rearward film-cooling, and (4) transpiration cooling. The vanes were tested over a range of coolant flow rates to about 6 percent of the primary flow at a primary- to coolant-total-temperature ratio of 1.0. Tests were conducted at pressure ratios that corresponded to mean-radius ideal aftermixed critical velocity ratios of 0.71 and 0.86. The design value for the vanes is 0.87. Overall vane efficiencies were obtained for these critical velocity ratios and compared, where possible, with the corresponding four-vane cascade results (cooling configurations 3 and 4). The efficiency and exit flow conditions as functions of radial position were also obtained and compared with the solid (uncooled) vane results. The results of this investigation are summarized as follows:

1. Increasing the coolant flow rate resulted in an increase in primary efficiency and a decrease in thermodynamic efficiency for all cooled vane configurations tested.

2. The primary efficiency was found to be independent of the ideal aftermixed critical velocity ratio, while the thermodynamic efficiency decreased with decreasing ideal aftermixed critical velocity ratio.

3. The thermodynamic efficiency as a function of radial position was found to be modified by the addition of coolant particularly near the end walls. No trend with coolant flow rate was noted for the aftermixed flow angle and aftermixed static- to inlet-total-pressure ratio.

4. Good agreement between the full-annular and four-vane-cascades results was obtained for the overall thermodynamic efficiency, but significant differences were noted for the overall primary efficiency.

5. For a given coolant flow rate, the highest overall efficiency was obtained for the trailing-edge-ejection vane and the lowest for the transpiration-cooled vane.

Lewis Research Center,
National Aeronautics and Space Administration,
Cleveland, Ohio, October 24, 1974,
505-04.

APPENDIX A

SYMBOLS

g	force-mass conversion constant, 32.174 lbm-ft/lbf-sec^2
$\overline{\overline{m}}$	total mass flow per passage, kg/sec (lbm/sec)
p	pressure, N/m^2 (lbf/ft^2)
R	gas constant, J/kg-K (ft-lbf/lbm-$^\circ$R)
r	radial position, m (ft)
T	temperature, K ($^\circ$R)
V	velocity, m/sec (ft/sec)
y	ratio of coolant flow to primary flow
y_c	ratio of coolant flow to total flow
y_p	ratio of primary flow to total flow
α	flow angle measured from axial direction, rad (deg)
γ	ratio of specific heats
$\overline{\eta}$	efficiency at radius r based on kinetic energy
$\overline{\overline{\eta}}$	overall efficiency based on kinetic energy
Θ	vane angular spacing, rad (deg)
θ	circumferential position, rad (deg)
ρ	density, kg/m^3 (lbm/ft^3)

Subscripts:

c	coolant flow
cr	flow condition at Mach 1
h	hub
i	survey position closest to inner (hub) wall
id	ideal or isentropic process
mean	mean radius
o	survey position closest to outer (tip) wall
p	primary flow

T	thermodynamic
t	tip
z	axial position
0	station at inlet plane of cascade bellmouth, fig. 2
1	station at vane inlet, fig. 2
2	station downstream of vane trailing edge, fig. 2
3	station downstream of vane trailing edge where survey measurements were taken, fig. 2
3M	station downstream of vane trailing edge where flow was assumed to be circumferentially mixed (uniform), fig. 2

Superscripts:

	total-state condition
(1)	leading-edge impingement coolant supply closed
(1+2)	leading-edge impingement coolant supply open

APPENDIX B

ESTIMATION OF AFTERMIXED EFFICIENCIES WITH LEADING-EDGE IMPINGEMENT COOLANT SUPPLY CLOSED

The performance results reported in reference 2 for the four-vane cascade were obtained with the leading-edge impingement coolant supply (fig. 4) open. Since there was no provision in the full-annular cascade for exhausting this coolant flow, the tests were conducted with the impingement supply sealed off. However, enough information is provided in reference 2 so that it is possible to estimate the performance that would have occurred in the four-vane cascade had the supply been closed. The basic assumption necessary to make this estimation is that at a constant coolant- to primary-total-pressure ratio, the only effect of having the leading-edge impingement coolant supply open is to increase the total coolant flow by the amount going through the leading-edge passage. This is reasonable since in reference 2 the leading-edge impingement coolant flow was mixed with the primary flow downstream of the survey plane and, therefore, did not affect the measured kinetic energy.

In order to estimate the performance with the impingement supply closed, the definitions of primary and thermodynamic efficiency (eqs. (7) and (1), respectively) were first written in the same form as used in reference 2. That is,

$$\overline{\eta}_{3M,p} = (1 + y)\frac{V_{3M}^2}{\left(V_{3M,id}\right)_p^2} \tag{B1}$$

$$\overline{\eta}_{3M,T} = \frac{(1 + y)\dfrac{V_{3M}^2}{\left(V_{3M,id}\right)_p^2}}{1 + y\dfrac{\left(V_{3M,id}\right)_c^2}{\left(V_{3M,id}\right)_p^2}} \tag{B2}$$

where the fraction of coolant flow to primary flow is given by

$$y = \frac{y_c}{y_p} \tag{B3}$$

Since the actual velocity has been assumed to be independent of whether the impingement coolant supply is open or closed and the ideal velocity of the primary stream was the same in both cases, the primary efficiency with the coolant supply closed $\bar{\eta}_{3M,p}^{(1)}$ and open $\bar{\eta}_{3M,p}^{(1+2)}$ is given, respectively, by

$$\bar{\eta}_{3M,p}^{(1)} = \left[1 + y^{(1)}\right] \frac{V_{3M}^2}{\left(V_{3M,id}\right)_p^2} \tag{B4}$$

$$\bar{\eta}_{3M,p}^{(1+2)} = \left[1 + y^{(1+2)}\right] \frac{V_{3M}^2}{\left(V_{3M,id}\right)_p^2} \tag{B5}$$

where $y^{(1)}$ and $y^{(1+2)}$ are the coolant fractions (at the same coolant- to primary-total-pressure ratio) with the impingement coolant supply closed and open, respectively. Therefore combining equations (B4) and (B5) gives

$$\bar{\eta}_{3M,p}^{(1)} = \left[\frac{1 + y^{(1)}}{1 + y^{(1+2)}}\right] \bar{\eta}_{3M,p}^{(1+2)} \tag{B6}$$

The performance with the holes open (i.e., $\bar{\eta}_{3M,p}^{(1+2)}$ and $y^{(1+2)}$) is given in reference 2. Also given are $y^{(1)}$ and $y^{(1+2)}$ as functions of coolant- to primary-total-pressure ratio. Therefore, the primary efficiency with the impingement coolant supply sealed off $\bar{\eta}_{3M,p}^{(1)}$ can be estimated from equation (B6). Similarly, the thermodynamic efficiencies can be written as

$$\bar{\eta}_{3M,T}^{(1)} = \frac{\left[1 + y^{(1)}\right] \dfrac{V_{3M}^2}{\left(V_{3M,id}\right)_p^2}}{1 + y^{(1)} \dfrac{\left(V_{3M,id}\right)_c^2}{\left(V_{3M,id}\right)_p^2}} = \frac{\bar{\eta}_{3M,p}^{(1)}}{1 + y^{(1)} \dfrac{\left(V_{3M,id}\right)_c^2}{\left(V_{3M,id}\right)_p^2}} \tag{B7}$$

$$\bar{\eta}_{3M,T}^{(1+2)} = \frac{\bar{\eta}_{3M,p}^{(1+2)}}{1 + y^{(1+2)} \dfrac{\left(V_{3M,id}\right)_c^2}{\left(V_{3M,id}\right)_p^2}} \tag{B8}$$

The ideal velocity of the coolant was the same in both cases since the coolant- to primary-total-pressure ratio was the same. Combining equations (B7) and (B8) gives

$$\bar{\eta}_{3M,T}^{(1)} = \frac{\bar{\eta}_{3M,p}^{(1)}}{1 + \dfrac{y^{(1)}}{y^{(1+2)}} \left[\dfrac{\bar{\eta}_{3M,p}^{(1+2)}}{\bar{\eta}_{3M,T}^{(1+2)}} - 1 \right]} \tag{B9}$$

REFERENCES

1. Gladden, Herbert J.; Dengler, Robert P.; Evans, David G.; and Hippensteele, Steven A.: Aerodynamic Investigation of Four-Vane Cascade Designed for Turbine Cooling Studies. NASA TM X-1954, 1970.

2. Stabe, Roy G.; and Dengler, Robert P.: Experimental Investigation of Aerodynamic Performance of Cooled Turbine Vanes at Gas-to-Coolant-Temperature Ratios Up to 2.75. NASA TM X-2733, 1973.

3. Goldman, Louis J.; and McLallin, Kerry L.: Cold-Air Annular-Cascade Investigation of Aerodynamic Performance of Cooled Turbine Vanes. I - Facility Description and Base (Solid) Vane Performance. NASA TM X-3006, 1974.

4. Prust, Herman W., Jr.; and Bartlett, Wayne M.: Cold-Air Study of the Effect on Turbine Stator Blade Aerodynamic Performance of Coolant Ejection from Various Trailing-Edge Slot Geometries. I - Experimental Results. NASA TM X-3000, 1974.

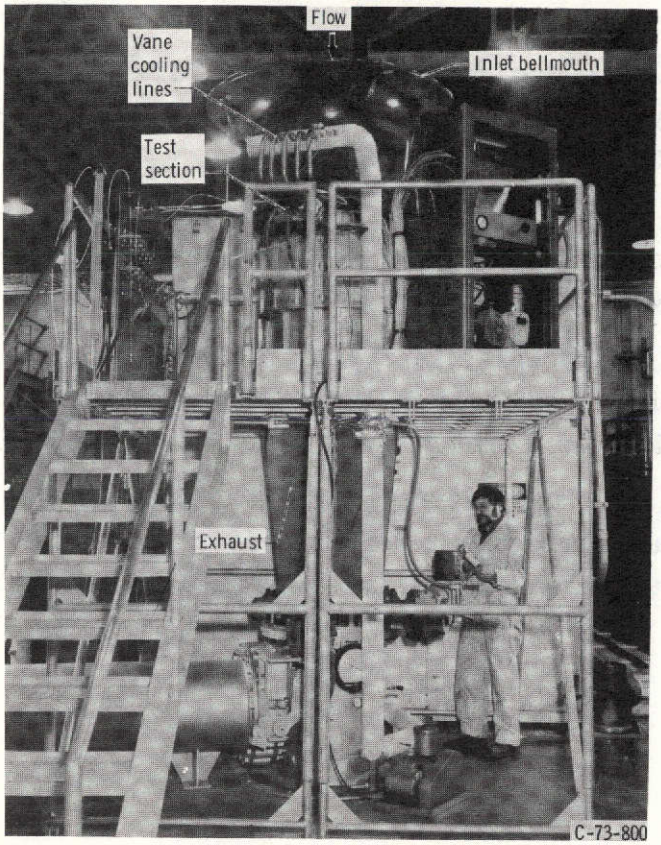

Figure 1. - Full-annular cascade.

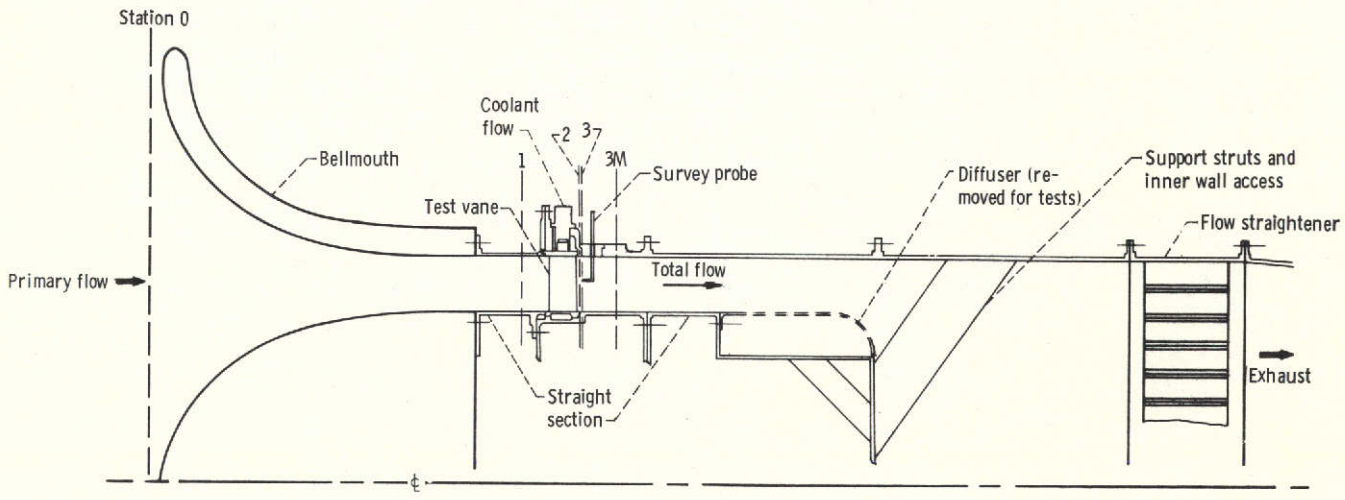

Figure 2. - Schematic cross-sectional view of 81-centimeter-diameter (32-in.) full-annular cascade.

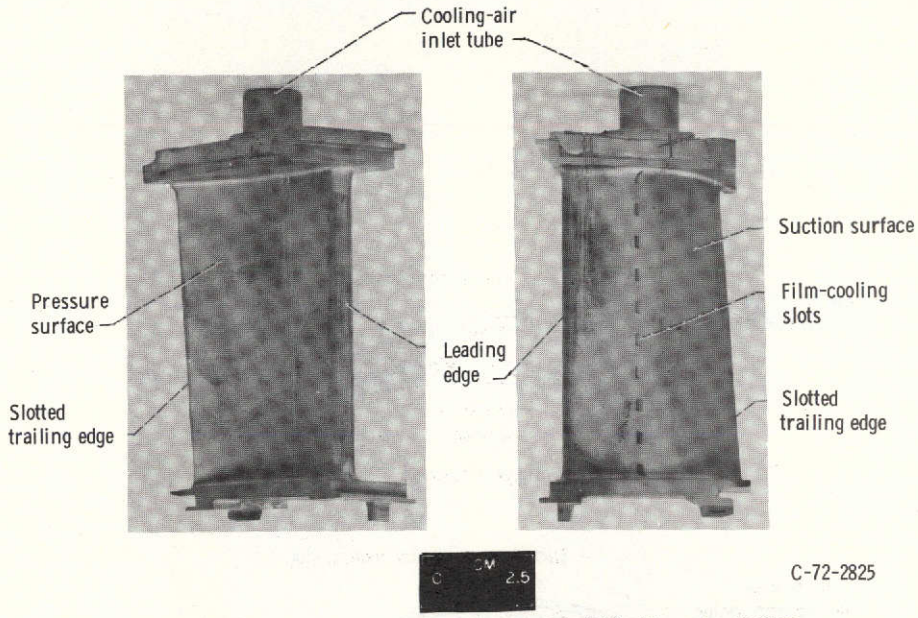

(a) Trailing-edge ejection.

(b) Trailing-edge ejection plus forward film-cooling.

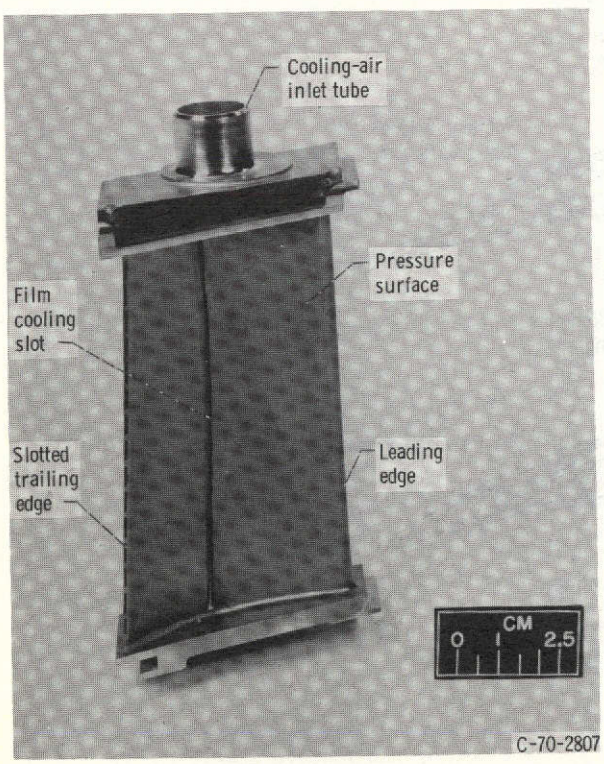

(c) Trailing-edge ejection plus rearward film-cooling.

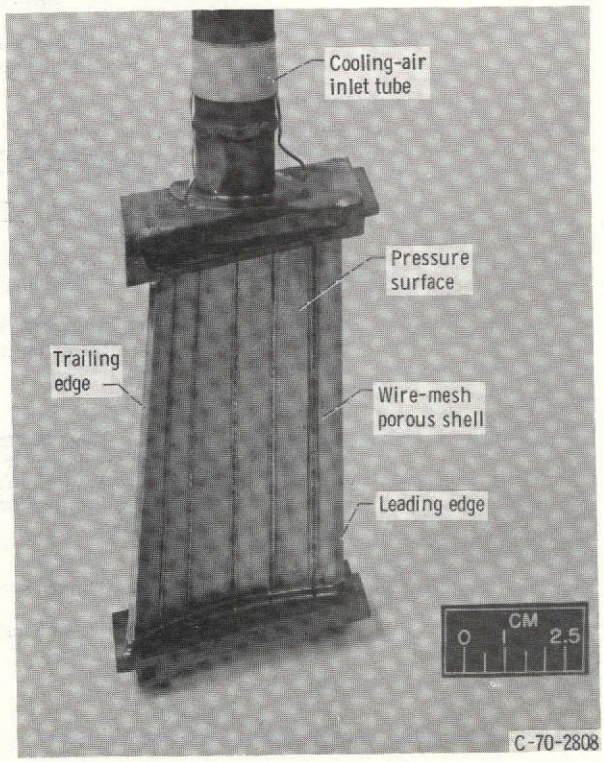

(d) Transpiration cooling.

Figure 3. - Air-cooled turbine stator vanes.

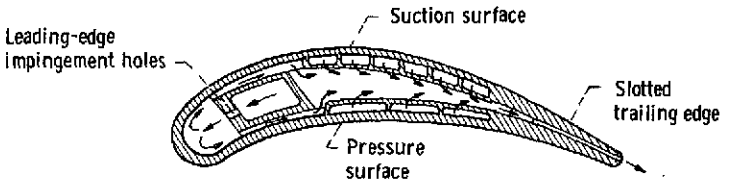

(a) Trailing-edge ejection.

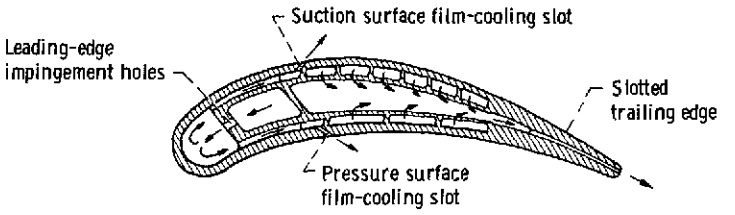

(b) Trailing-edge ejection plus forward film-cooling.

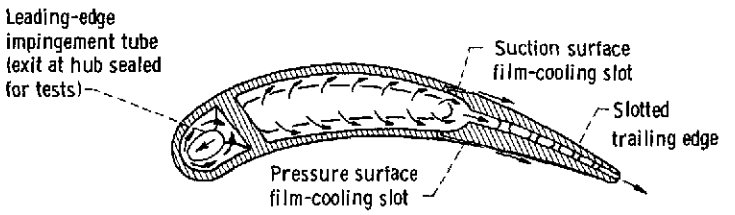

(c) Trailing-edge ejection plus rearward film-cooling.

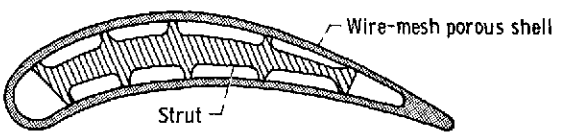

(d) Transpiration cooling.

Figure 4. - Cross-sectional view of cooled vanes.

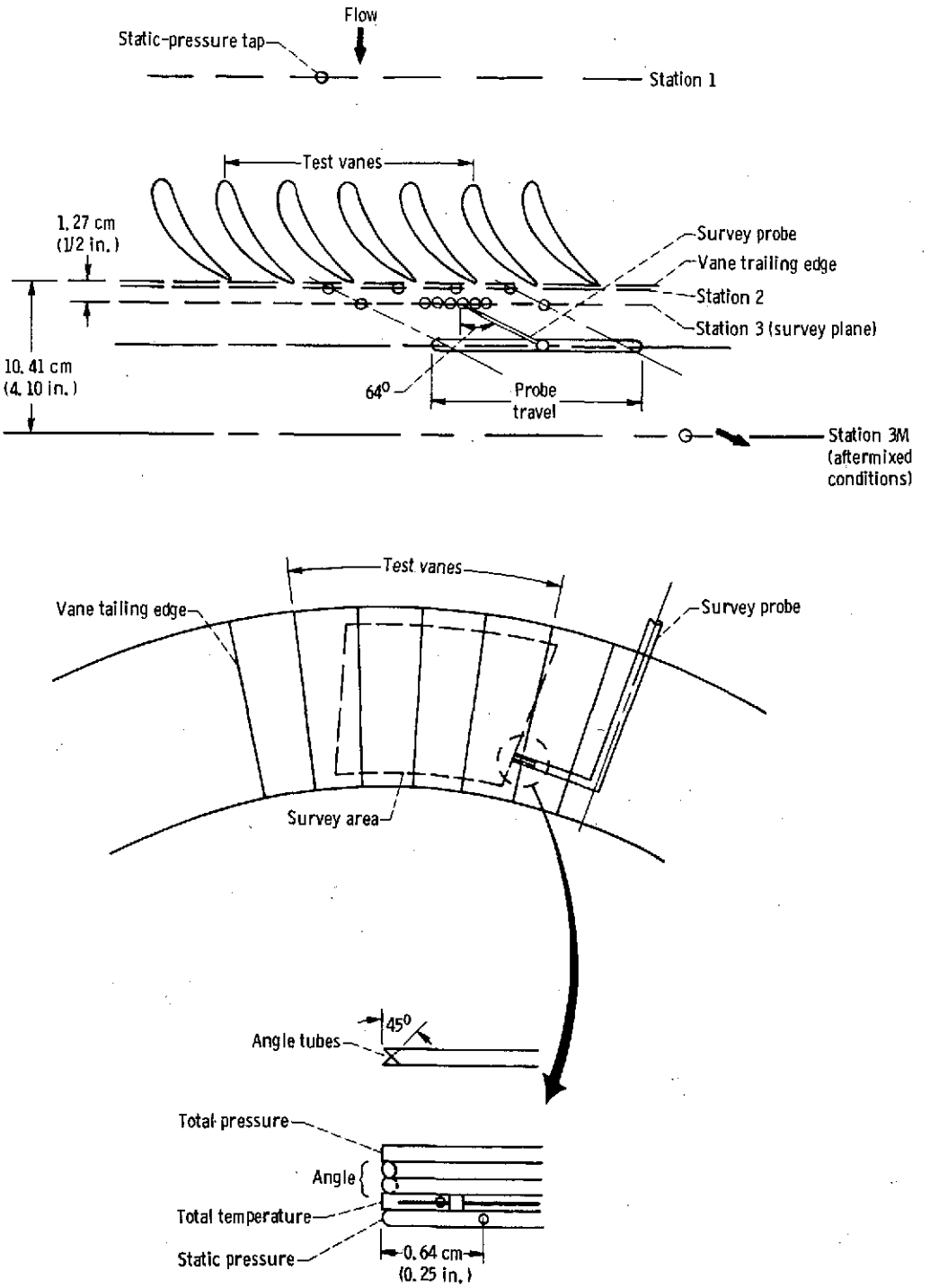

Figure 5. - Schematic of instrumentation for survey data.

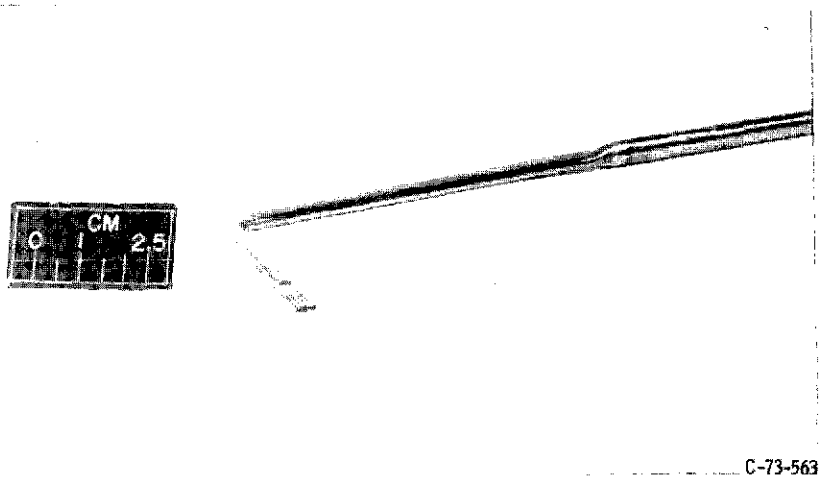

Figure 6. - Survey probe.

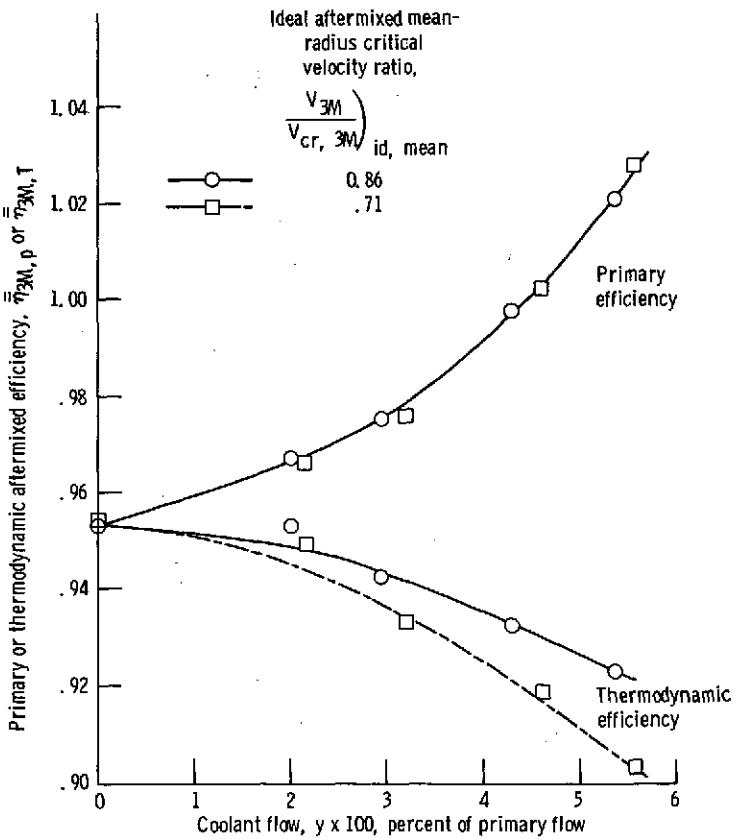

Figure 7. - Variation of efficiency with coolant flow and ideal aftermixed critical velocity ratio for trailing-edge-ejection cooling vanes.

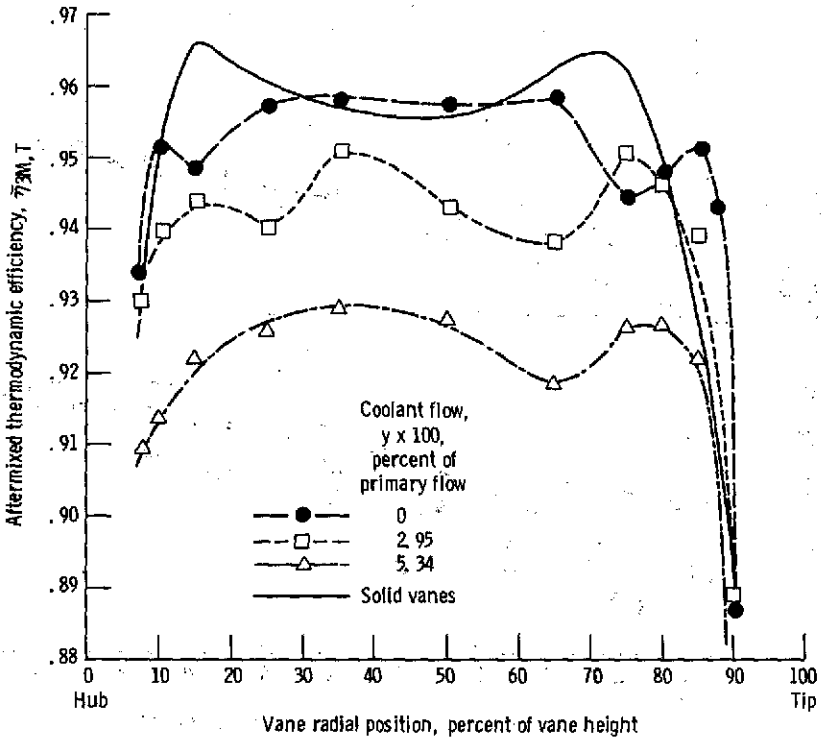

Figure 8. - Variation of efficiency with radial position and coolant flow for trailing-edge-ejection cooling vanes at 0.86 ideal aftermixed critical velocity ratio.

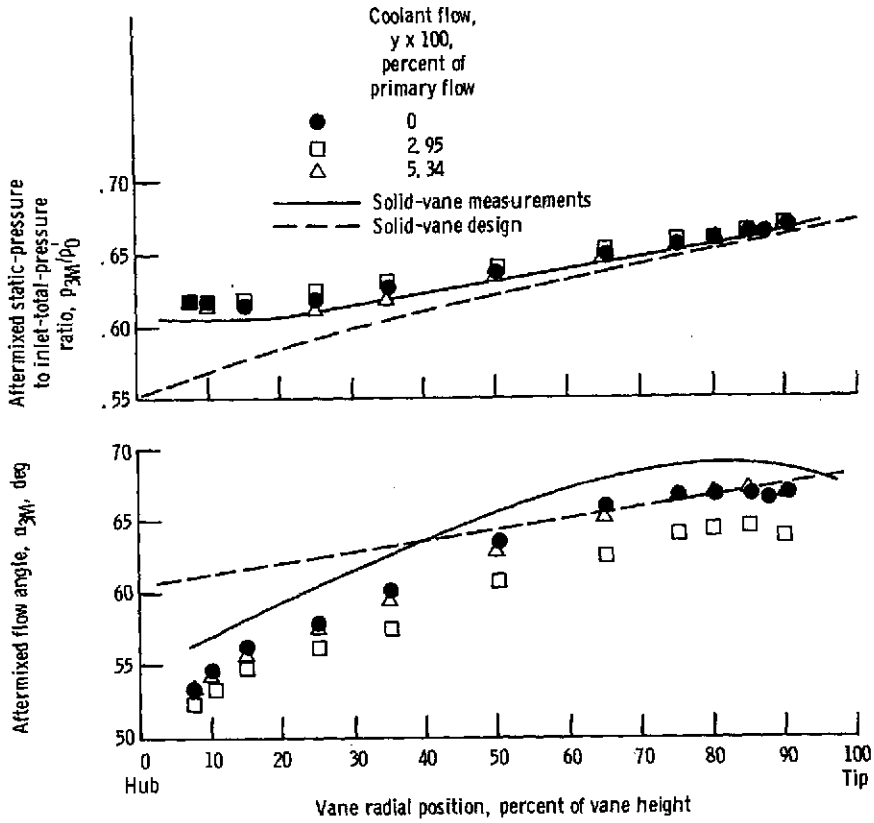

Figure 9. - Variation of aftermixed flow angle and aftermixed static-pressure to inlet-total-pressure ratio with radial position and coolant flow for trailing-edge-ejection cooling vanes at 0.86 ideal aftermixed critical velocity ratio.

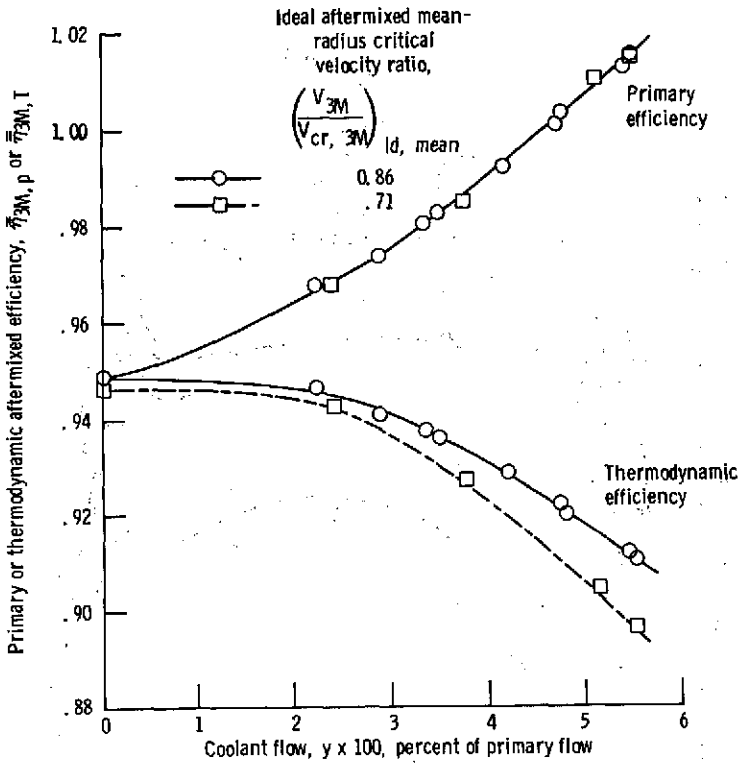

Figure 10. - Variation of efficiency with coolant flow and ideal aftermixed critical velocity ratio for vanes with trailing-edge ejection plus forward film-cooling.

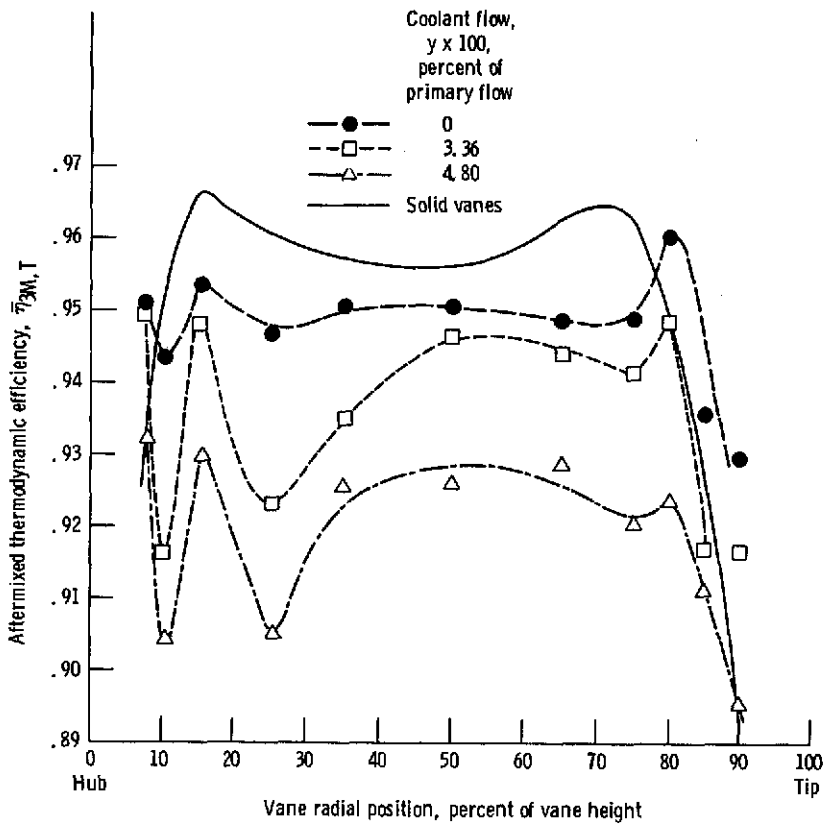

Figure 11. - Variation of efficiency with radial position and coolant flow for vanes with trailing-edge ejection plus forward film-cooling at 0.86 ideal aftermixed critical velocity ratio.

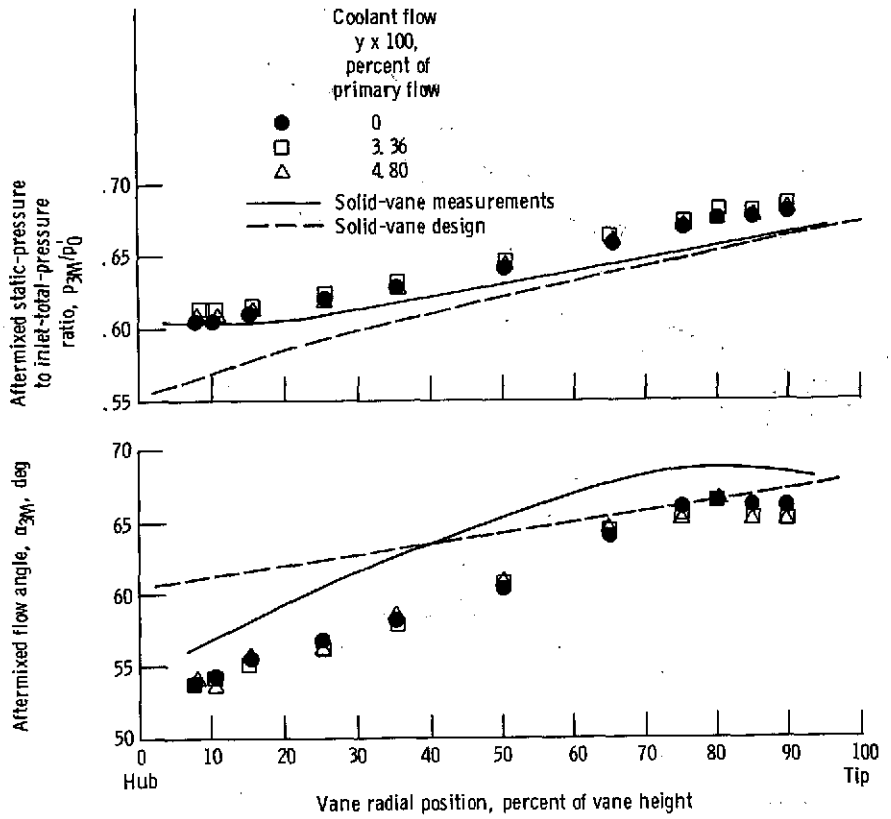

Figure 12. - Variation of aftermixed flow angle and aftermixed static-pressure to inlet-total-pressure ratio with radial position and coolant flow for vanes with trailing-edge ejection plus forward film-cooling at 0.86 ideal aftermixed critical velocity ratio.

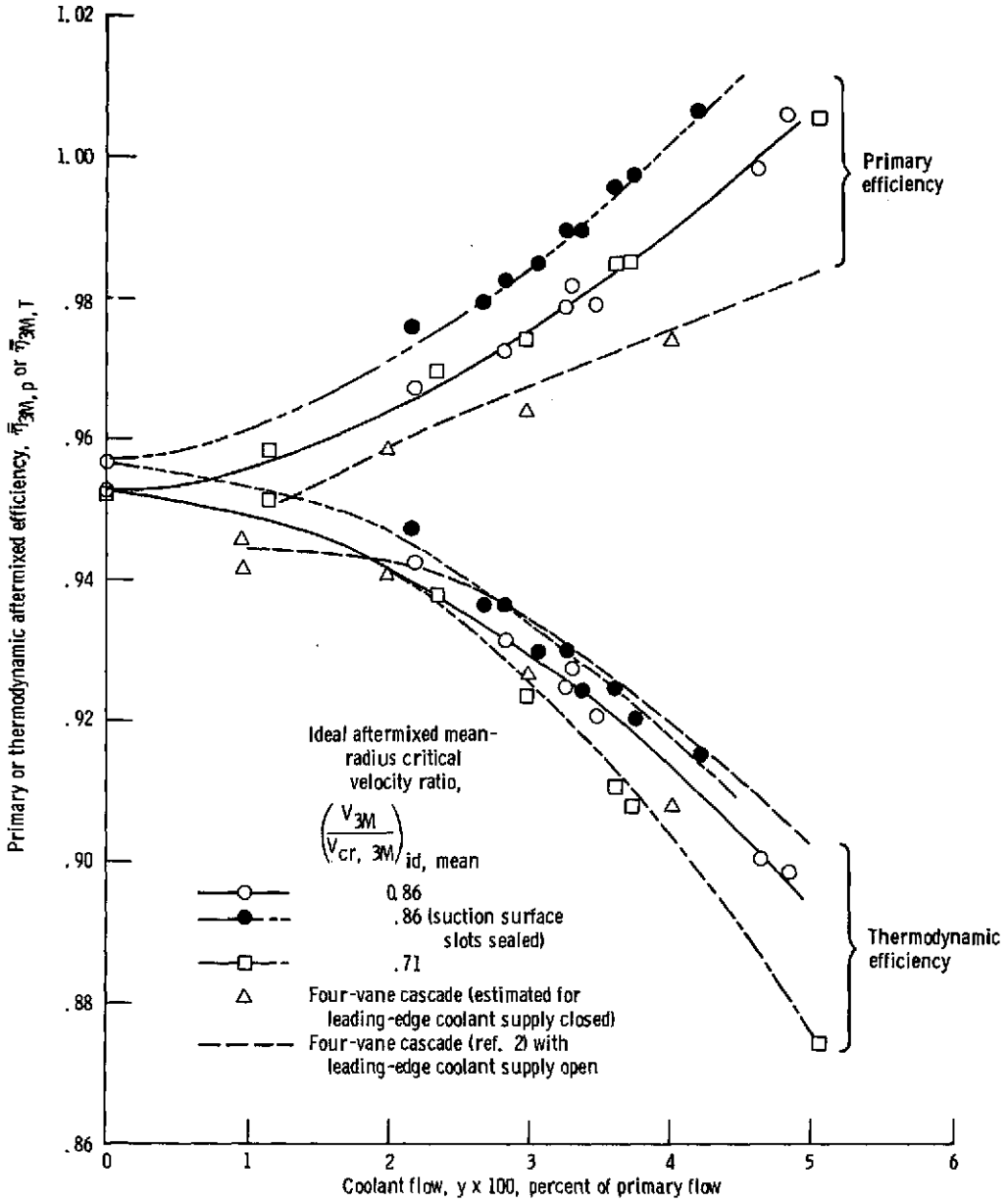

Figure 13. - Variation of efficiency with coolant flow and ideal aftermixed critical velocity ratio for vanes with trailing-edge ejection plus rearward film-cooling.

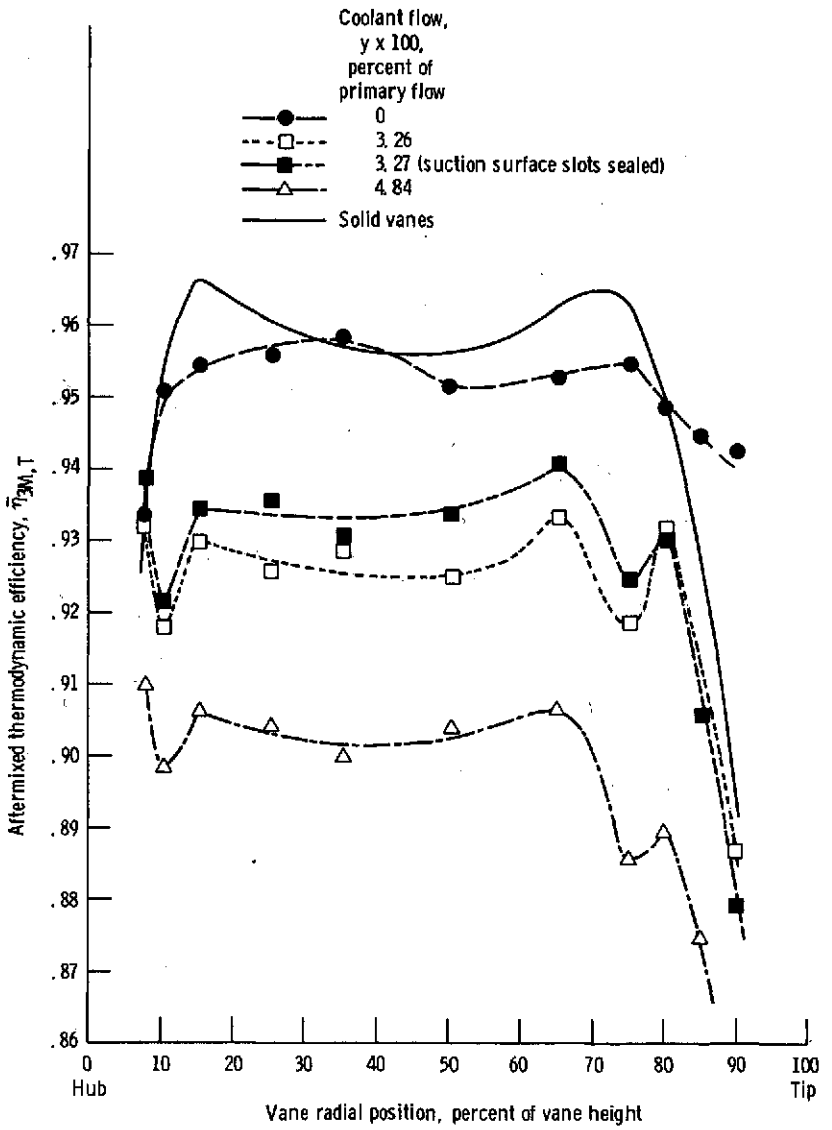

Figure 14. - Variation of efficiency with radial position and coolant flow for vanes with trailing-edge ejection plus rearward film-cooling at 0.86 ideal aftermixed critical velocity ratio.

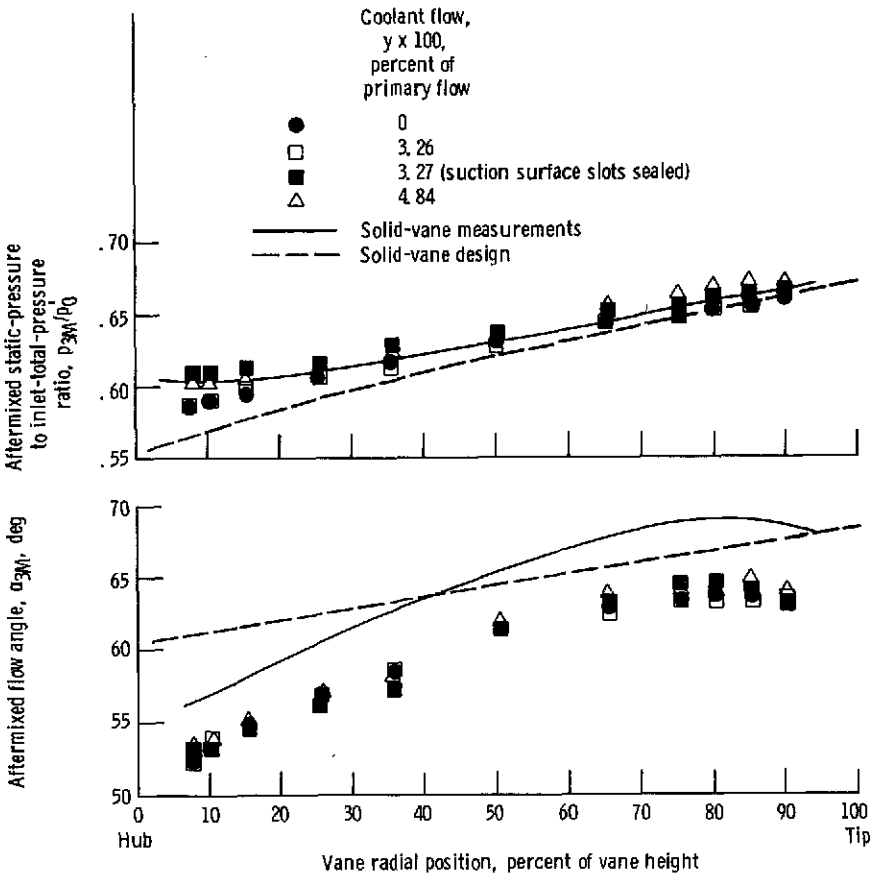

Figure 15. - Variation of aftermixed flow angle and aftermixed static-pressure to inlet-total-pressure ratio with radial position and coolant flow for vanes with trailing-edge ejection plus rearward film-cooling at 0.86 ideal aftermixed critical velocity ratio.

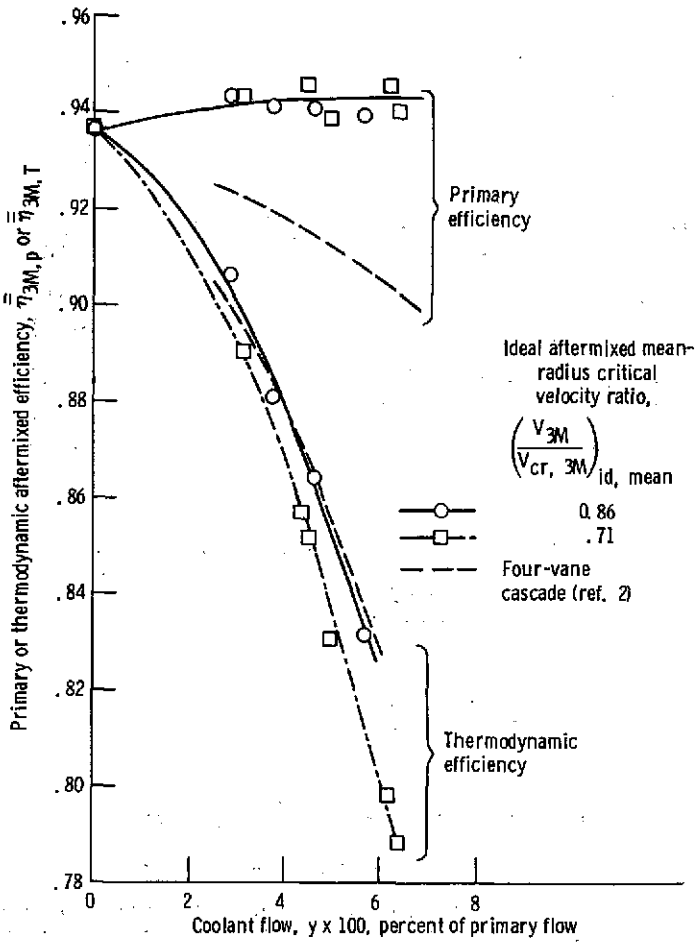

Figure 16. - Variation of efficiency with coolant flow and ideal aftermixed critical velocity ratio for transpiration-cooled vanes.

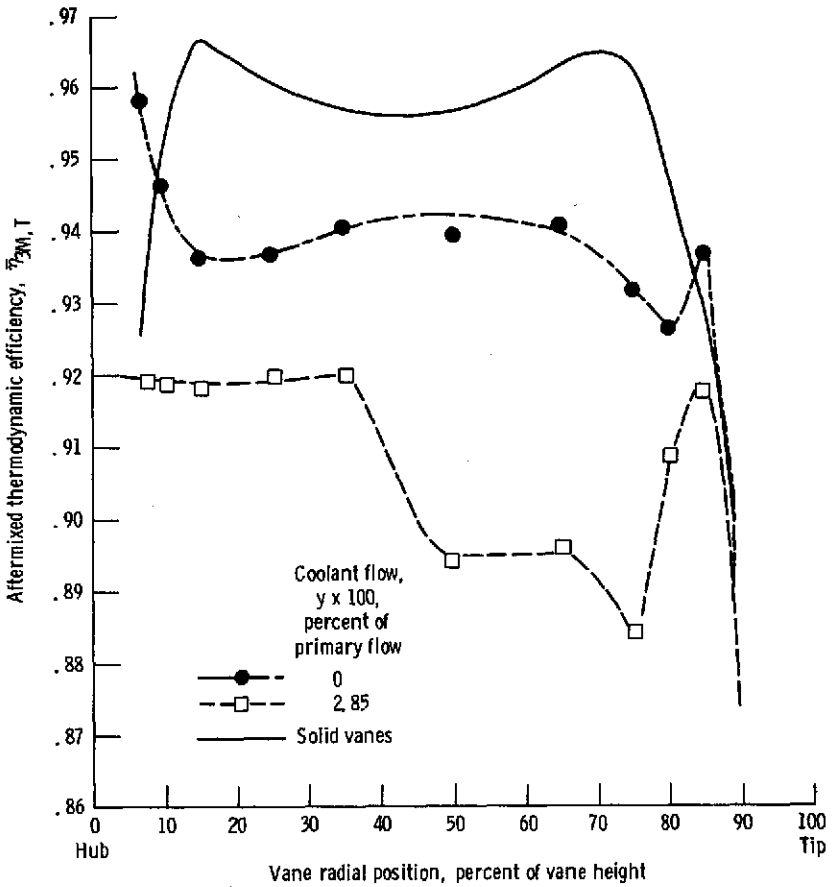

Figure 17. - Variation of efficiency with radial position and coolant flow for transpiration-cooled vanes at 0.86 ideal aftermixed critical velocity ratio.

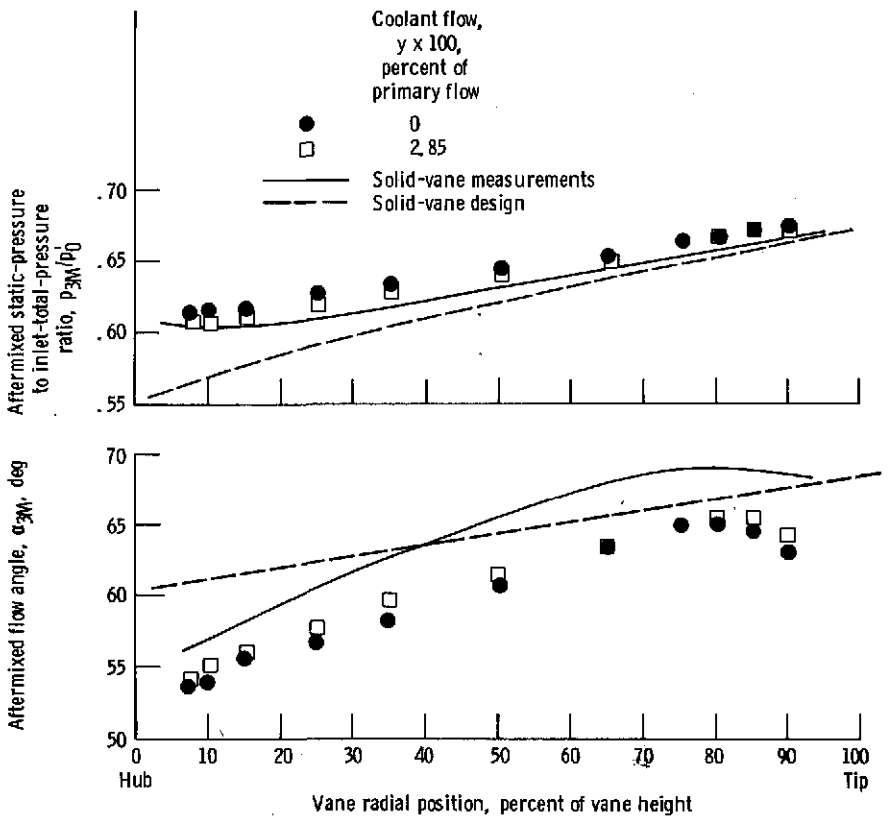

Figure 18. - Variation of aftermixed flow angle and aftermixed static-pressure to inlet-total-pressure ratio with radial position and coolant flow for transpiration-cooled vanes at 0.86 ideal aftermixed critical velocity ratio.

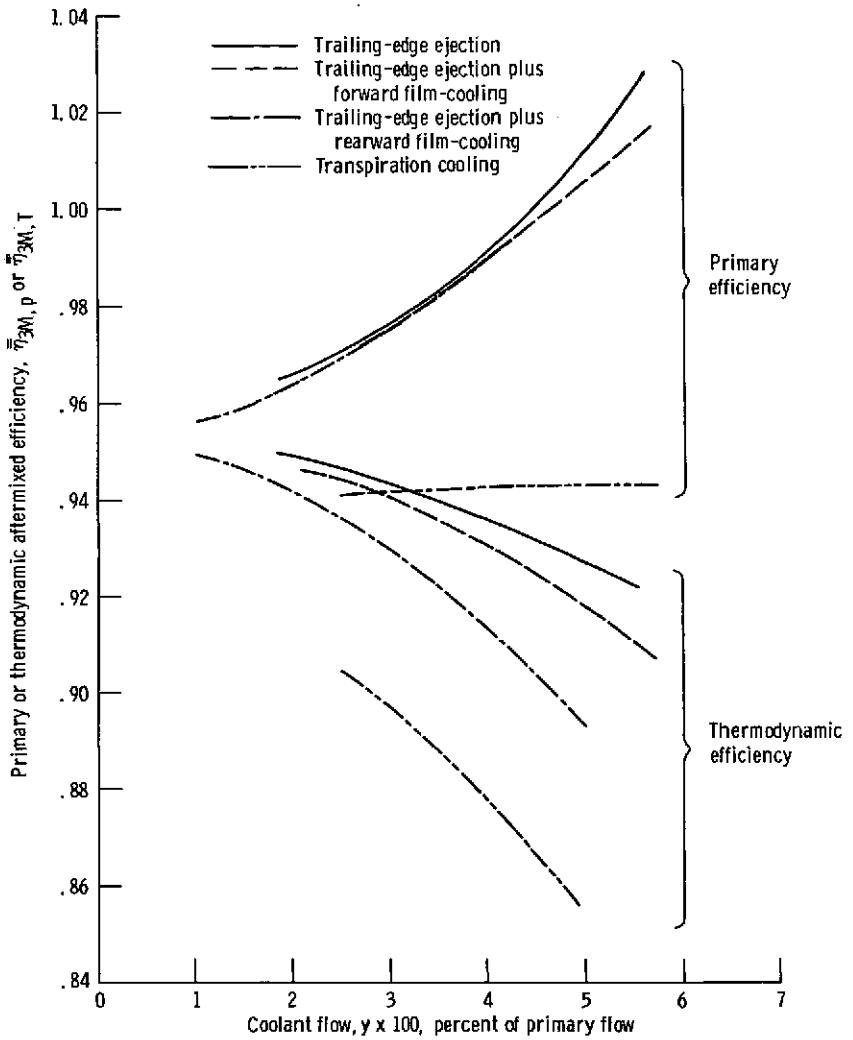

Figure 19. - Variation of efficiency with coolant flow for different vane cooling configurations at 0.86 ideal aftermixed critical velocity ratio.

NASA-Langley, 1975 E-8049